

# Femtosecond Laser-induced Crystallization of Amorphous Indium Tin Oxide Film on Glass Substrate for Patterning Applications

Chung-Wei Cheng\*<sup>1</sup>, Yi-Ju Lee\*<sup>2</sup>, Wei-Chih Shen\*<sup>1</sup>, Jenq-Shyong Chen\*<sup>2</sup> and Chin-Wei Chien\*<sup>1</sup>

\*<sup>1</sup> ITRI South, Industrial Technology Research Institute, No. 8, Gongyan Rd., Liujia Shiang, Tainan County 734, Taiwan, R.O.C.

E-mail: CWCheng@itri.org.tw

\*<sup>2</sup> Department of Mechanical Engineering, National Chung Cheng University, No. 168, University Rd., Min-Hsiung, Chia-Yi 621, Taiwan, R.O.C.

A method is proposed for patterning crystalline indium tin oxide (c-ITO) structures on amorphous ITO (a-ITO) thin films using a femtosecond laser. In the proposed approach, the a-ITO film is transformed into a c-ITO film over a predetermined area of the glass substrate via the heat energy supplied by the laser beam and the unirradiated a-ITO film is then removed using an acidic etchant solution. The c-ITO patterns are observed using scanning electron microscopy (SEM). The results confirm that the pattern width can be precisely controlled via an appropriate selection of the repetition rate, laser power and scanning speed. In addition, the experimental results show that a high repetition rate (80 MHz) reduces the thermal cycling effect and yields a corresponding improvement in the surface properties of the c-ITO patterns.

**Keywords:** femtosecond laser, ITO, crystalline, patterning, heat accumulation effect

## 1. Introduction

In order to improve the device characteristics of optoelectronic products such as flat-panel displays and solar cells, the amorphous materials used in the fabrication of such products are transformed into a crystalline material via a thermal annealing process in order to reduce their resistivity and enhance their transparency. Indium tin oxide (ITO) is one of the most widely-used transparent conducting materials, and thus the development of rapid and precise crystalline ITO (c-ITO) patterning techniques has attracted significant interest in recent decades.

Conventionally, c-ITO patterns are fabricated via the photolithography of an amorphous ITO (a-ITO) thin film followed by a thermal annealing process [1]. However, this approach has the disadvantages of multiple and high-cost processes. Thus, the feasibility of using a direct laser ablation technique to pattern the ITO film by removing the undesired portion of the thin film has significant appeal. As a result, the literature contains many investigations into the application of both long-pulse (i.e. nanosecond) [2-9] and ultra-fast pulse (i.e. picosecond or femtosecond) [10-12] laser systems for patterning purposes. The ablation process requires a finite amount of laser fluence to evaporate the workpiece material, and thus conventional long-pulse lasers result in the formation of elevated ridges at the edge of the ablation path and defects in the layers below. Even the use of ultra-fast pulse lasers does not necessarily preclude the formation of elevated ridges or the presence of ITO residue at the base of the ablated channel. In [13-14], the authors utilized a nanosecond excimer laser to pattern a-ITO films via a crystallization effect. However, the results showed that the thermal effects induced by the relatively long laser pulse degraded the patterning precision. Moreover, the laser crystallization process required the use

of a patterning mask, and thus the minimum attainable line pitch was constrained by the optic diffraction limit of the mask.

Accordingly, this study proposes a novel two-step technique for fabricating c-ITO patterns using a femtosecond laser-induced crystallization process. In the proposed approach, the desired area of the ITO film is transformed from an amorphous structure to a crystalline structure via laser irradiation. The patterned ITO film is then etched in an oxalic acid solution to remove the unwanted a-ITO regions. The crystallization effect is examined under different irradiation conditions, i.e. different repetition rates, laser energies, scanning speeds, and so on. It is shown that given an appropriate choice of irradiation parameters, the patterning process can be accomplished without the need for a mask or a subsequent thermal annealing process.

## 2. Experimental

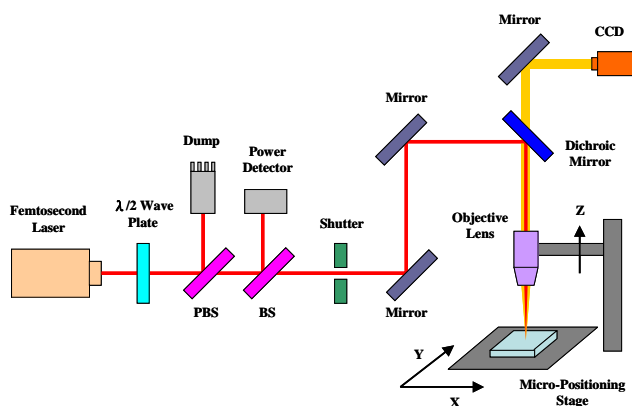
In the present experiments, a-ITO thin films with a thickness of approximately 100 nm were deposited on glass substrates (NEG OA10) using a DC magnetron sputtering system. The crystallization experiments were performed using two different femtosecond lasers, namely (1) a regenerative amplified mode-locked Ti:sapphire laser (SPIT FIRE, Spectra-Physics) with a low repetition rate of 1 kHz, a pulse duration of ~120 fs, a central wavelength of 800 nm, and a maximum pulse energy of ~3.5 mJ; and (2) an oscillator-only Ti:sapphire laser (Mai-Tai, Spectra-Physics) with a high repetition rate of 80 MHz, a pulse duration of ~100 fs, a central wavelength of 800 nm, and a maximum pulse energy of ~100 nJ.

Figure 1 presents a schematic illustration of the experimental setup. As shown, the energy of the linear

polarized Gaussian laser beam was attenuated initially by a rotatable half-wave ( $\lambda/2$ ) plate and a polarizing beam splitter (PBS). The laser energy was measured by passing the polarized light beam through a beam splitter (BS) and routing the reflected component to a power detector. Meanwhile, the transmitted laser beam was passed through a shutter and a reflective mirror system such that it entered an objective lens (numerical aperture 0.26, M Plan Apo NIR, Mitutoyo) and was incident in the normal direction on the surface of the a-ITO coated specimen mounted on an X-Y axis stage. For both lasers, the focal spot size on the surface of the ITO films was adjusted to a diameter of approximately  $\sim 5 \mu\text{m}$ .

The c-ITO structures were fabricated by translating the sample stage in the X- and Y-directions under the control of a PC-based micro-positioning system with an accuracy of better than  $1 \mu\text{m}$ . The scanning speed was varied in the range  $0.05\sim 0.5 \text{ mm/s}$  for the low repetition rate femtosecond laser and  $10\sim 50 \text{ mm/s}$  for the high repetition rate femtosecond laser. The fabrication process was monitored continuously via a charge-coupled device (CCD) camera.

After the laser-induced crystallization process, the samples were immersed in a  $0.1 \text{ N}$  oxalic acid etchant at  $50^\circ\text{C}$  for  $2.5 \text{ min}$ . Note that the required etching time was determined by using a multimeter to check for an electrical resistance of greater than  $20 \text{ M}\Omega$  between adjacent c-ITO structures, thereby confirming the complete removal of the original a-ITO film. After etching, the samples were observed by scanning electron microscopy (SEM, FE-SEM 7001).



**Fig. 1** Schematic illustration showing experimental setup used for femtosecond laser patterning of a-ITO films

### 3. Results and Discussion

#### 3.1 Patterning experiments with low repetition rate femtosecond laser (1 kHz)

Figure 2(a) presents a microscope image showing the line patterns fabricated on an a-ITO thin film surface using a laser power of  $50 \mu\text{W}$  ( $50 \text{ nJ}$ ) and scanning speeds of  $0.05$ ,  $0.25$ , and  $0.5 \text{ mm/s}$ , respectively. Note that the specimen is in an unetched condition and the lines were patterned with the laser beam linearly polarized in a direction perpendicular to the scan direction. It can be seen that the film within the laser-irradiated area is slightly different from that within the unirradiated region. The irradiated sample was then etched, leaving a clear line pattern on the glass sub-

strate, see Fig. 2(b). Figures 2(c)~(e) present high-magnification SEM images of the line patterns from Fig. 2 (b). In every case, the lines are found to have a width of around  $1.5 \mu\text{m}$ . This result indicates that the etching rate of the laser-irradiated line pattern is much lower than that of the a-ITO thin film, and thus the unirradiated ITO is removed without any significant erosion of the irradiated ITO patterns. The irradiated ITO pattern is presumed to be crystalline since the etching rates of a- and c-ITO are very different [13].

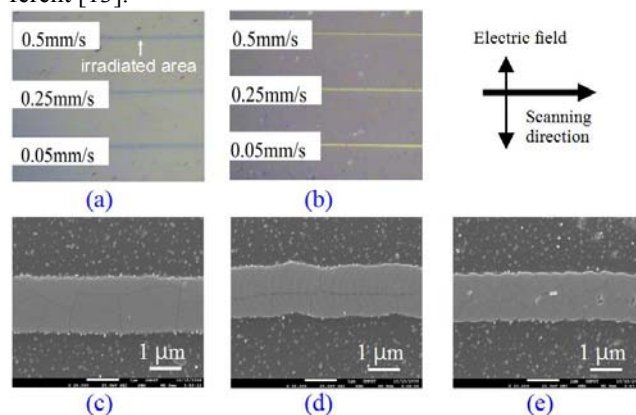


**Fig. 2** (a)~(b) Microscope images of irradiated a-ITO thin film surfaces before and after etching, respectively. (c)~(e) SEM images showing line patterns fabricated at different scanning speeds, i.e. (c)  $0.05 \text{ mm/s}$ , (d)  $0.25 \text{ mm/s}$ , and (e)  $0.5 \text{ mm/s}$ .

Figure 3 presents SEM images of the c-ITO line patterns produced by the low repetition laser at a scanning speed of  $0.25 \text{ mm/s}$  and laser powers in the range  $40\sim 90 \mu\text{W}$ . Note that in performing the patterning process, the laser beam was linearly polarized in a direction parallel to the scan profile. Due to the Gaussian property of the beam profile, the middle of each line is irradiated by a higher laser energy than the edges. In the c-ITO line patterns shown in Figs. 3(a) and 3(b), corresponding to laser powers of  $40 \mu\text{W}$  and  $50 \mu\text{W}$ , respectively, the peak energy intensity of the laser beam is higher than the crystallization threshold, but lower than the ablation threshold. In Figs. 3(c) and 3(d), the peak energy intensity of the laser beam is close to the ablation threshold, and thus a ripple-like characteristic is observed along the center line of the c-ITO patterns. Finally, in Figs. 3(e) and 3(f), corresponding to laser powers of  $80 \mu\text{W}$  and  $90 \mu\text{W}$ , respectively, the peak energy intensity of the laser beam is higher than the ablation threshold, and thus the center of the c-ITO line is ablated.

Figures 3(a)~(d) show that at lower values of the laser power, i.e.  $40\sim 70 \mu\text{W}$ , the line patterns contain a large number of micro-cracks. As will be discussed later in Section 3.2, this suggests that the laser repetition rate ( $1 \text{ kHz}$ ) is too low for the a-ITO material to generate a heat accumulation effect in the a-ITO film between successive laser pulses, and thus the film experiences a strong thermal cycling effect.

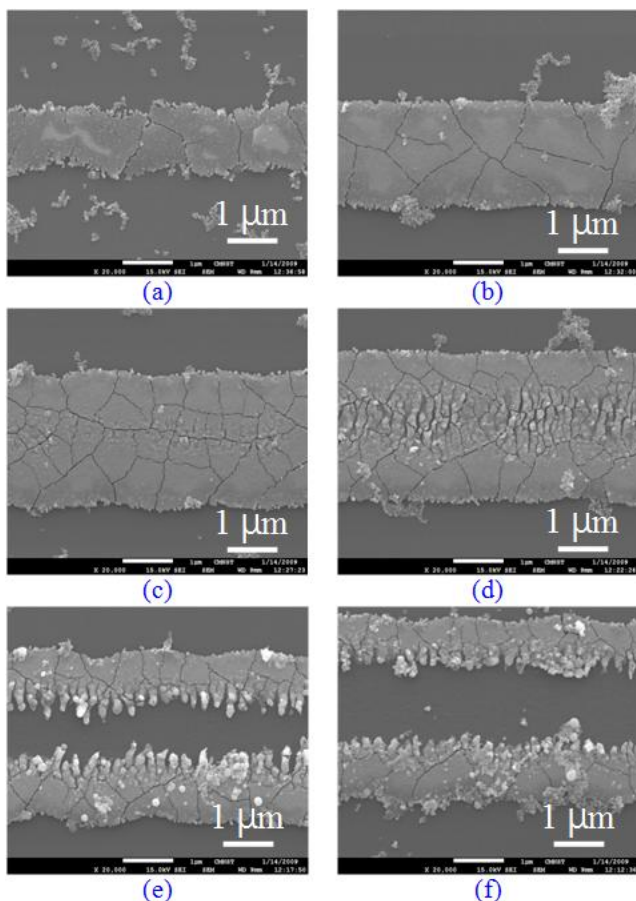


**Fig. 3** SEM images of c-ITO line patterns fabricated with laser beam linearly polarized in direction parallel to scan direction and laser powers of: (a) 40μW, (b) 50μW, (c) 60μW, (d) 70μW, (e) 80μW, and (f) 90μW. Note that scanning speed is 0.25 mm/s in every case.

In Figs. 3(a)~(d), the pattern widths are seen to be sensitive to the spatial intensity distribution of the focused laser beam. Assuming a Gaussian incident beam profile, the pattern width  $W$  is related to the irradiation laser energy  $E$  by

$$W^2 = 2\omega_e^2 \ln(E/E_{th}) \quad (1)$$

where  $E_{th}$  is the multiple pulse crystallization threshold energy and  $\omega_e$  is the effective beam radius at the interaction surface. Figure 4 illustrates the variation of the pattern width with the laser energy as a function of the scanning speed. The straight lines obtained by curve fitting the experimental data confirm the logarithmic dependence between the pattern width and the laser energy (see Eq. (1)). Moreover, the crystallization threshold is seen to be in the region of 30~40 nJ. Table 1 summarizes the estimated crystallization threshold energy, fitting-line gradient, effective beam diameter, and correlation coefficient for each of the three scanning speeds shown in Fig. 4. It is observed that a low scanning speed (i.e. a high number of laser pulses applied to the same spot) results in a lower crystallization threshold energy. This result is consistent with the incubation phenomenon reported by Krüger and Kautek [15]. In addition, the average slope of the fitting line is found to be around 7, while the average effective beam diameter is approximately 4 μm, i.e. similar to the theoretical focus spot size 5 μm.

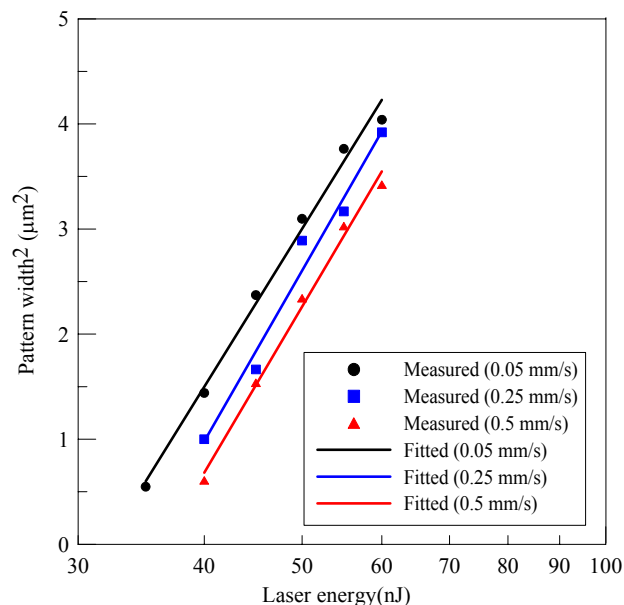


**Fig. 4** Variation of pattern width with laser energy as function of scanning speed

**Table 1** Comparison of crystallization characteristics of low repetition rate femtosecond laser (1 kHz)

Scanning speed (mm/s)	Crystallization threshold energy, $E_{th}$ (nJ)	Fitting line gradient, $2\omega_e^2$	Effective beam diameter, $2\omega_e$ (μm)	Correlation coefficient
0.05	32.02	6.73	3.67	0.9922
0.25	34.96	7.27	3.81	0.9768
0.5	36.32	7.07	3.76	0.9929

### 3.2 Patterning experiments with high repetition rate femtosecond laser (80 MHz)

Figure 5 presents SEM images of the c-ITO line patterns fabricated using the high repetition rate femtosecond laser with a constant scanning speed of 30 mm/s and laser powers in the range 210~360 mW. It can be seen that the c-ITO lines are free of the micro-cracks shown in Fig. 3 and have a smooth, unblemished surface characteristic. Thus, it appears that the high repetition rate femtosecond laser results in a more uniform crystallization effect than that achieved using the low repetition rate laser.

It has been reported that the processing of certain bulk transparent glasses using a high repetition rate femtosecond laser (i.e. a frequency greater than 200 kHz) prompts a heat accumulation effect, which minimizes the thermal cycling phenomenon between successive laser pulses and prevents collateral damage [16]. When the time between successive laser pulses is shorter than the heat diffusion time, e.g. 1 μs for a 1 μm<sup>3</sup> volume of typical fused silica, the energy input to the irradiated specimen by successive pulses accumulates within the focal volume and prompts a significant increase in the local temperature. The thermal cycling effect is therefore avoided because the local temperature remains at a high, fairly constant value throughout the annealing process rather than increasing / decreasing cyclically.

The results presented in Fig. 5, suggest that such a heat accumulation effect is also present in the a-ITO thin film specimens processed using the current high repetition rate (80 MHz) femtosecond laser. The effective cooling time of the a-ITO specimens is around 21 μs, i.e.  $t_c = d_v^2/D$  [17], where  $d_v$  is the diameter of the focused laser beam spot (~ 5 μm) and  $D$  is the thermal diffusivity of a-ITO (~  $1.2 \times 10^{-6}$  m<sup>2</sup>/s). This value of  $t_c$  is much larger than the time interval between successive pulses, i.e. 0.012 μs for an 80 MHz repetition rate, and thus a significant temperature accumulation effect occurs within the local region of the specimen. However, in the low repetition rate experiments, the value of  $t_c$  is much smaller than the time interval between successive pulses, i.e. 1 ms for a 1 kHz repetition rate. As a result, the temperature within the crystallization area drops significantly between laser pulses. In other words, the low repetition rate results in an obvious thermal cycling effect, which prompts the formation of the micro-cracks shown in the c-ITO patterns presented in Figs. 3(a)~(d).

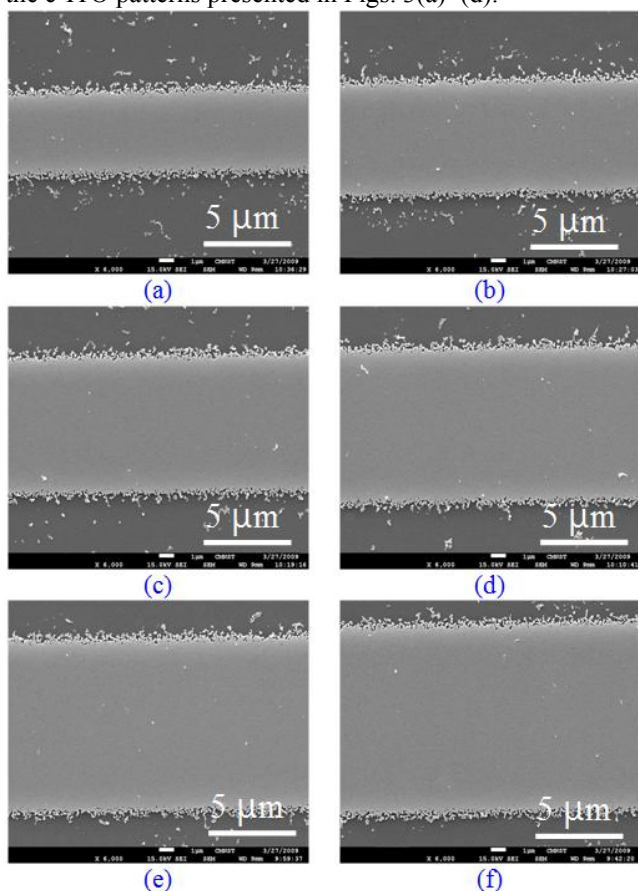


**Fig. 5** SEM images of c-ITO line patterns fabricated with laser beam linearly polarized in direction parallel to scan direction and laser powers of: (a) 210mW, (b) 240mW, (c) 270mW, (d) 300mW, (e) 330mW, and (f) 360mW. Note that scanning speed is 30 mm/s in every case.

To investigate the heat accumulation effect and crystallization threshold of a-ITO thin films fabricated using a high repetition rate femtosecond laser, c-ITO line patterns were produced using laser powers in the range 210~360 mW and scanning speeds of 10, 30 and 50 mm/s, respectively. As shown in Fig. 5, the pattern width is sensitive to the spatial intensity distribution of the focused laser beam. In evaluating the heat accumulation effect, the effective

beam radius term  $\omega_e$  in Eq. (1) is replaced by  $\omega_{e,h}$ , which is equal to the approximate summation of the focused beam radius and the extended width caused by the heat accumulation effect. The straight lines obtained by curve fitting the experimental data once again confirm the logarithmic relationship between the pattern width and the laser energy. Table 2 summarizes the estimated crystallization threshold energy, fitting line gradient, effective beam diameter and correlation coefficient for each of the scanning speeds shown in Fig. 6. It is observed that a lower scanning speed results in a lower annealing threshold energy and a higher effective beam diameter. Furthermore, in contrast to the results presented in Table 1 for the low repetition rate experiments, it can be seen that the fitting line gradient decreases significantly with an increasing scanning speed. In other words, the extended width caused by the heat accumulation effect becomes less at higher values of the scanning speed.

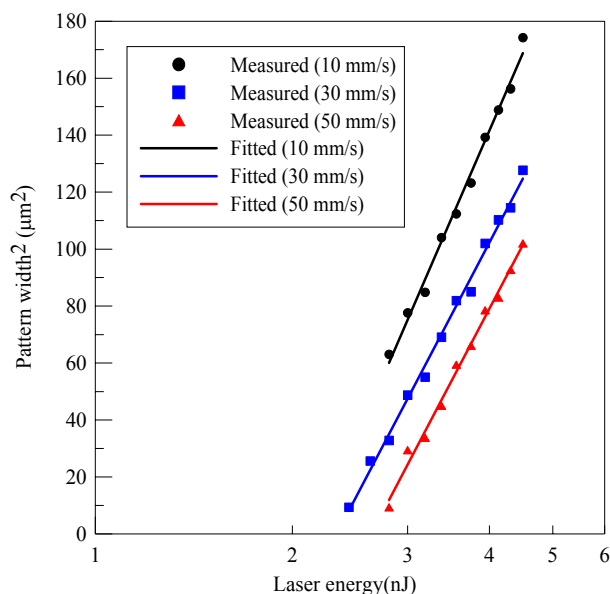


**Fig. 6** Variation of pattern width with laser energy as function of scanning speed

**Table 2** Comparison of crystallization characteristics of high repetition rate femtosecond laser (80 MHz)

Scanning speed (mm/s)	Crystallization threshold energy, $E_{th}$ (nJ)	Fitting line gradient, $2\omega_{e,h}^2$	Effective beam diameter, $2\omega_{e,h}$ (μm)	Correlation coefficient
10	2.08	215.02	20.74	0.9927
30	2.33	190.49	19.52	0.9945
50	2.62	186.20	19.30	0.9936

**4. Conclusions**

This study has presented an approach for the patterning of c-ITO structures on glass substrates using a laser-induced crystallization process. The experimental results have demonstrated that the line width of the c-ITO patterns can be precisely controlled via a careful control of the laser irradiation parameters. Moreover, the etching procedure

ensures that the regions of the glass substrate between the c-ITO patterns are completely free of ITO residues, and thus the problem of electrical shorting is avoided. Overall, the experimental results presented in this study confirm that the proposed laser patterning technique provides a versatile and highly precise means of fabricating the transparent electrode structures required in a wide range of modern optoelectronic devices.

#### Acknowledgements

We thank Costas P. Grigoropoulos, David Jen Hwang, and Juen-Kai Wang for useful discussion. In addition, we would like to appreciate the support from the Ministry of the Economic Affairs (MOEA), Taiwan, R.O.C. for performing this project.

#### References

- [1] H. Morikawa and M. Fujita, "Crystallization and electrical property change on the annealing of amorphous indium-oxide and indium-tin-oxide thin," *Thin Solid Films*, Vol. 359, 2000.
- [2] O. Yavas et al., "Effect of substrate absorption on the efficiency of laser patterning," *J. Appl. Phys.*, Vol. 85, 1999.
- [3] R. Tanaka et al., "Laser etching of indium tin oxide thin films by ultra-short pulsed laser," *Proc. of SPIE*, Vol. 5063, 2003.
- [4] D. Ashkenasi et al., "Fundamentals and advantages of ultrafast micro-structuring of transparent materials," *Appl. Phys. A*, Vol. 77, 2003.
- [5] C. Molpeceres et al., "Microprocessing of ITO and a-Si thin films using ns laser sources," *J. Micromech. Microeng.*, Vol. 15, 2005.
- [6] J.H. Kim, "The analysis of ablation on ITO thin film for 1064nm irradiation," *Proc. of the 4th International Congress on Laser Advanced Materials Processing*, 2006.
- [7] N. Fukuda, "Development of DPSS-laser-based ITO patterning system," *ICALEO Congress Proceeding*, 2006.
- [8] M. Henry et al., "Laser direct write of active thin-films on glass for industrial flat panel display manufacture," *Proc. of the 4th International Congress on Laser Advanced Materials Processing*, 2006.
- [9] M.Y. Xu et al., "F<sub>2</sub>-laser patterning of indium tin oxide (ITO) thin film on glass substrate," *Appl. Phys. A*, Vol. 75, 2006.
- [10] M. Park et al., "Ultrafast laser ablation of indium tin oxide thin films for organic light-emitting diode application," *Optics and Lasers in Engineering*, Vol. 44, 2006.
- [11] I.B. Sohn et al., "Femtosecond laser patterning of ITO film for display panel," *Proc. of the 4th International Congress on Laser Advanced Materials Processing*, 2006.
- [12] Gediminas RAČIUKAITIS et al., "Patterning of ITO layer on glass with high repetition rate picosecond lasers," *Journal of Laser Micro/Nanoengineering*, Vol. 2, 2007.
- [13] H. Hosono et al., "Excimer laser crystallization of amorphous indium-tin-oxide and its application to fine patterning," *Jap. J. Appl. Phys.*, Vol. 37, 1998.
- [14] Y.H. Son et al., "Excimer laser crystallization of a-ITO thin film deposited on plastics," *J. Korean Phys. Soc.*, Vol. 42, 2003.
- [15] J. Krüger and W. Kautek, "Ultrafast pulse laser interaction with dielectrics and polymers," *Adv. Polymer Sci.*, Vol. 168, 2004.
- [16] R.R. Gattass et al., "Micromachining of bulk glass with bursts of femtosecond laser pulses at variable repetition rates," *Opt. Express*, Vol. 14, 2006.
- [17] S. Juodkazis et al., "Thermal accumulation effect in three-dimensional recording by picosecond pulses," *Appl. Phys. Lett.*, Vol. 85, 2004.

(Received: June 4, 2009, Accepted: October 26, 2009)